Clays and Clay Minerals, Vol. 40, No. 1, 103–113, 1992.

EFFECTS OF LAYER CHARGE, CHARGE LOCATION, AND ENERGY CHANGE ON EXPANSION PROPERTIES OF DIOCTAHEDRAL SMECTITES

TSUTOMU SATO,[1] TAKASHI WATANABE,[2] AND RYOHEI OTSUKA[1]

[1] Department of Mineral Resources Engineering, School of Science and Engineering, Waseda University
Okubo, Shinjuku-ku, Tokyo, 169 Japan

[2] Department of Geoscience, Joetsu University of Education
Yamayashiki, Joetsu, Niigata, 943 Japan

Abstract—Expansion properties of ten homoionic smectites that differed in amount and location of layer charge were examined by X-ray powder diffraction analysis at various relative humidities, or after glycerol or ethylene glycol solvations. Except for K-samples with glycerol solvation, and Na- and Ca-samples with ethylene glycol, differences in the basal spacings are observed in samples having similar layer charge. These results show that the basal spacings are larger when the layer charge is located in octahedral sites than when it is in tetrahedral sites. This suggests that expansion is due to the combined effects of the charge location and amount.

The effects of layer charge magnitude and location on expansion were represented by an energy change (*expansion energy:* ΔEr) during the hydration and solvation processes. Plots of basal spacings versus ΔEr show a reasonable relationship; the spacings generally decrease stepwise as the value of ΔEr increases. The basal spacings of K-samples with glycerol solvation, Na-saturated and K-saturated samples at 100% RH are apt to contract stepwise with increasing value of ΔEr. For these samples, the figures showing the relationship between each expanded phase and the charge characteristics are obtained from the isoquants of ΔEr, given the boundary of the expanded phases. A behavior test using these figures may be combined with the Greene-Kelly test to estimate the amount and the location of the layer charge of common smectites.

Key Words—Charge location, Ethylene glycol, Expanded phase, Expansion energy, Glycerol, Layer charge, Relative humidity, Smectite.

INTRODUCTION

Differences in expansion properties of montmorillonites, beidellites, and vermiculites have been of interest to clay mineralogists. Many workers have studied the relationship between expansion properties and crystallographic factors. Mooney *et al.* (1952) and Keren and Shainberg (1975) find that variation in basal spacing depends chiefly on the kind and valency of the interlayer cations. Iwasaki (1979) and Iwasaki and Watanabe (1988) support this view on the basis of the expansion behavior of smectites. Schultz (1969) and Horváth and Novák (1976), on the other hand, claim that the total layer charge is the controlling factor influencing expansion properties. Brindley (1966) and Suquet *et al.* (1975) determined the basal spacings of ethylene glycol (EG) and glycerol complexes (GLY) of smectite and vermiculite with various layer charges and concluded that the total layer charge plays a major role in the expansion properties of layer silicates. However, the precise relationship between layer charge and expansion is still not clear. For example, Kodama *et al.* (1974), Suquet *et al.* (1975, 1977), and Watanabe and Sato (1988) reported that expandable clay minerals with the same layer charge had different expansion behaviors. Glaeser and Mering (1968) and Suquet *et al.* (1975, 1977) estimated the effects of interlayer cations, net layer charge, and charge location (octahedral or tetrahedral) on the expansion properties. From their investigation of a synthetic smectite, Harward and Brindley (1965) insisted that beidellite exhibits expansion properties intermediate between those of montmorillonite and vermiculite. In these papers, it was generally found that the basal spacings of tetrahedrally-charged smectites were smaller than those of the octahedrally-charged smectites under the same hydration and solvation conditions. Jenkins and Hartman (1979, 1982) considered all possible factors influencing the expansion properties of layer silicates, and calculated the electrostatic contribution to the interlayer bonding. They concluded that the energy required to expand the octahedrally-charged layer silicate was larger than that of the tetrahedrally-charged layer silicate. On the other hand, Schultz (1969) suggested that the expansion properties did not depend on the charge location. In these papers there is discrepancy with respect to the factors that affect the expansion of smectites. It is very important for better identification and characterization of the expandable clay minerals to elucidate the cor-

Table 1. Location and characteristics of studied samples.

Sample	Location	Charge distribution[3] Tetrahedral	Charge distribution[3] Octahedral	Total[3]	d(060) (Å)	Data source
SWy-1[1] montmorillonite	Crook County, Wyoming	0.16	0.52	0.68	1.499[4]	Jaynes and Bigham (1987)
N1[2] montmorillonite	Mizumaki, Fukuoka Pref.	0.28	0.40	0.68	1.498[4]	Iwasaki and Watanabe (1988)
TU6[2] montmorillonite	Tsukinuno, Yamagata Pref.	0.48	0.32	0.80	1.499[4]	Iwasaki and Watanabe (1988)
Ts[2] montmorillonite	Tsukinuno, Yamagata Pref.	0.14	0.78	0.92	1.499[4]	Nagasawa (1988)
Sta-9c[2] montmorillonite	sediment core from northeastern Pacific	0.02	0.84	0.86	1.509	Aoki (1974)
M6[2] montmorillonite	Matsuki, Akita Pref.	0.22	0.72	0.94	1.498[4]	Iwasaki and Watanabe (1988)
SAz-1[1] montmorillonite	Apache County, Arizona	0.14	1.00	1.14	1.499[4]	Jaynes and Bigham (1987)
NG-1[1] nontronite	Hohen Hagen, Germany	0.72	0.04	0.76	ind.[4]	Malla and Douglas (1987)
BS-3[2] beidellite	Sano, Nagano Pref.	1.00	0.12	1.12	1.494	Matsuda (1988)
B2[2] beidellite	Unterrupsroth, Germany	0.75	0.42	1.17	n.o.	Nadeau *et al.* (1985)

ind. = indeterminate, n.o. = not observed.
[1] CMS samples (obtained from the Source Clay Repository of The Clay Minerals Society).
[2] Samples provided by T. Iwasaki (N1, TU6 and M6), K. Nagasawa (Ts), S. Aoki (Sta-9c), T. Matsuda (BS-3) and M. J. Wilson (B2).
[3] Calculated for $O_{20}(OH)_4$.
[4] Data obtained from this study.

relation between the various factors and the expansion properties.

At present, based on previous studies, the identification of the expandable clay minerals is generally based on the expanding behavior of samples saturated with either Ca or Mg and solvated with either ethylene glycol or glycerol (Walker, 1958; Harward *et al.*, 1969), and on the collapsing behavior of K-saturated samples (Weaver, 1956). These expanding-behavior tests have been widely used for distinguishing the different expandable minerals. However, these tests are not diagnostic for the estimation of charge characteristics in common smectites in which the charge is distributed over tetrahedral and octahedral sheets.

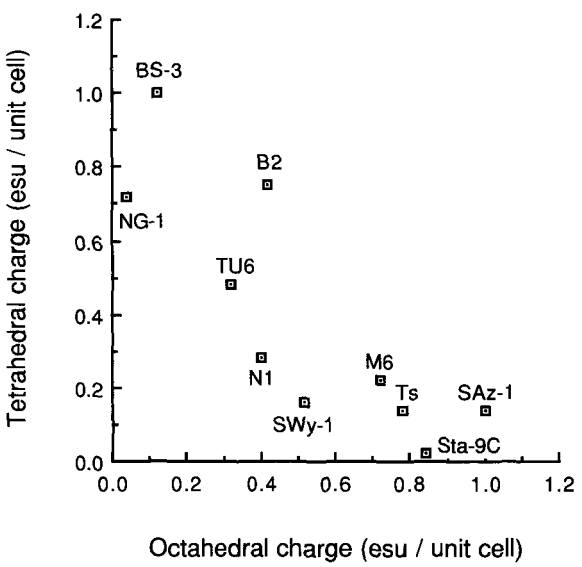

Figure 1. Charge distribution of studied samples. Tetrahedral and octahedral charge are calculated for $O_{20}(OH)_4$. The charge values listed are for a unit cell which is $O_{20}(OH)_4$.

The objectives of this paper, therefore, are (1) to explore the respective effects of net layer charge and charge location on the expansion properties of dioctahedral smectites, and (2) to establish the principal criteria useful for the estimation of charge characteristics.

MATERIALS AND EXPERIMENTAL METHODS

Samples

Ten smectites were examined in this study. Some characteristics of the samples are given in Table 1. Mineralogically, these smectites consist of six montmorillonites (Sta-9c, SWy-1, SAz-1, N1, M6, and Ts), one nontronite (NG-1), and three beidellites (TU6, BS-3, B2). The value of the d_{060} spacing indicates that all the samples are dioctahedral (Table 1). These samples are considerably different in net layer charge (within the range from 0.68 to 1.17 esu/unit cell) and in the relative amounts of negative charge in the octahedral and tetrahedral layers. The charge distributions of these samples are presented in Figure 1 as plots of tetrahedral charge versus octahedral charge (esu/unit cell).

https://doi.org/10.1346/CCMN.1992.0400111 Published online by Cambridge University Press

Sample preparation

All samples were ultrasonically disaggregated in distilled water and the <2-μm fraction separated using centrifugation. The separates were air-dried at room temperature. Homoionic M-clays (M = Li^+, Na^+, K^+, and Ca^{2+}) were prepared by treating the colloidal fractions with 1 N chloride solutions, except for the Ca^{2+}-clays which were prepared using a 1 N acetate solution. The clays were treated with the salt solutions three times at 24 hour intervals. Afterward, the clays were treated two more times with the salt solutions to achieve complete exchange. Then, they were washed three times with 80% ethanol and several times with distilled water until chloride free. For XRD investigation, oriented specimens were prepared by drying the suspensions on glass slides at room temperature.

For the Greene-Kelly test, Li-saturated samples were prepared with water and spread on silica slides. The samples were allowed to dry slowly at room temperature and then heated at 250°C for 24 hr in a muffle furnace. Afterward, for solvation, the slides were placed in a sealed glass container containing glycerol for 24 hr.

X-ray diffraction

The oriented XRD patterns of the homoionic samples were measured under a controlled relative humidity (RH) and also after solvation with glycerol (GLY) or ethylene glycol (EG). XRD examination under controlled RH was performed by the ReCX (*Re*lative humidity *C*ontrol system for *X*-ray diffractometer). The ReCX system was described in detail by Watanabe and Sato (1988). Using this system, the following experiment was performed. The oriented samples were kept in the specimen chamber at 0% RH for 6 hours. Then, XRD examination was performed at 10% RH intervals in the range of 0–100% RH after confirming that a constant d-spacing and intensity of the (001) reflection had been obtained at each RH. It took up to 10 minutes to reach equilibrium after each 10% RH increment. Only the hydration process (0–100% RH) was used because the hydration and the dehydration curves of smectite are not the same (Keren and Shainberg, 1975). Solvation with GLY or EG was accomplished by the vapor pressure method (Brunton, 1955; Brown and Farrow, 1956). The samples were saturated with GLY vapor at 110°C for up to 24 hr and with EG vapor at 60°C for up to 24 hr. The samples were then exposed for varying lengths of time up to a maximum of 20 days. The change of d-spacings and the intensity of the (001) reflection of solvated samples was not confirmed. The XRD patterns were obtained with a Rigaku diffractometer (RAD-IIA) using monochromatized CuKα radiation. The XRD patterns were recorded from 2°–50°2θ with a resolution of 0.05°2θ.

RESULTS AND DISCUSSION

Greene-Kelly test

The Greene-Kelly test (Greene-Kelly, 1953a, 1953b, 1955) was applied to the samples in this study. Samples Ts, SAz-1, and Sta-9c collapsed irreversibly, which indicates that the sites of isomorphic substitution are mainly in the octahedral layer. Samples NG-1, BS-3, and B2 showed a basal spacing of about 17.8 Å with integral secondary spacing; the isomorphic substitution sites are, therefore, largely in the tetrahedral layer. The XRD patterns of samples SWy-1, N1, TU6, and M6 have nonintegral basal reflections. These patterns are interpreted as a random or segregated-type interstratification of collapsed layers (about 9.5 Å) and expanded layers (about 17.8 Å). In order to estimate the proportion of beidellitic components, observed XRD patterns made after the Greene-Kelly test were compared with calculated patterns produced by a computer program for simulation of the (00*l*) diffraction profiles of a one-dimensionally disordered crystal [Watanabe (1981), and modified by T. Iwasaki (personal communication)]. The proportions of tetrahedral charge (see Table 1) calculated from structural formulae were approximately consistent with those of the beidellite component obtained from the computer estimation.

Expansion with ethylene glycol (EG)

Charge characteristics and basal spacings of EG-solvated samples are summarized in Table 2. Three stages were observed: two homogeneous stages with basal spacings of about 17 Å and 14 Å, and an intermediate stage with basal spacings between 17 Å and 14 Å.

Except for the K-saturated NG-1, SAz-1, BS-3, B2 samples, the basal reflections of the EG-solvated samples showed integral basal reflections with a basal spacing of about 17 Å. This suggests that a homogeneous bilayer, EG-smectite complex had formed (Brindley, 1966).

The basal reflections of the K-saturated SAz-1, BS-3, and B2 samples showed an integral series with a basal spacing of about 14 Å, which corresponds to one-layer of EG molecules. This phase was recognized only in the K-saturated samples with a high net layer charge. Suquet *et al.* (1977) reported that K-saturated trioctahedral minerals with a net layer charge >1.0 (esu/unit cell) did not expand to 17 Å with EG solvation. Machajdik and Čičel (1981) suggested that the net layer charge of K-smectites needed for the formation of 14 Å and 17 Å phases was 1.0–1.6 and 0.5–1.2 (esu/unit cell), respectively. Our data indicate that K-smectites (except for NG-1) with layer charges of 0.68–0.94 (esu/unit cell) form 17 Å bilayer complexes with EG, and that K-smectites with layer charge of 1.12–1.17 (esu/unit cell) form 14 Å monolayer complexes.

Table 2. Layer charge and basal spacings (Å) of ethylene glycol- and glycerol-solvated smectites.

Sample[1]	Layer charge		Ethylene glycol solvation			Glycerol solvation		
	Total	Tetrahedral	Na	K	Ca	Na	K	Ca
SWy-1	0.68	0.16	17.20	17.34	17.18	18.18	(14.73)	17.92
N1	0.68	0.28	17.10	17.20	17.18	18.05	14.15	17.93
NG-1	0.76	0.72	16.95	(15.78)	16.87	18.14	(14.03)	17.88
TU6	0.80	0.48	17.00	17.20	16.90	18.12	(14.03)	17.83
Sta-9c	0.86	0.02	17.32	16.99	16.98	18.03	(14.54)	17.90
Ts	0.92	0.14	16.95	17.33	16.83	17.90	14.00	17.93
M6	0.94	0.22	17.10	16.90	17.10	17.91	(13.66)	17.72
BS-3	1.12	1.00	17.09	14.07	16.76	17.45*	(13.72)	17.37*
						14.35*		14.58*
SAz-1	1.14	0.14	16.97	13.90	16.86	17.90	(13.68)	17.78
B2	1.17	0.75	16.87	13.74	16.76	(16.61)	(13.27)	17.69

Values in parentheses are obtained from only (001) reflection of nonintegral series.
Asterisks indicate the subordinate reflections for doubly-expanded phases having different spacings.
[1] See Table 1 for sources of samples.

A nonintegral series of reflections with a basal d-spacing between about 14 Å and 17 Å was observed for K-saturated NG-1. The nonintegral and asymmetrical reflections indicate a random interstratification between monolayer and bilayer EG complexes. The glycolated, K-saturated, NG-1 sample has a layer charge of 0.76 and has an unexpectedly smaller d_{001} spacing than those of the other low-charge smectites. This is probably due to the strong electrostatic forces between the interlayer cations and the negative charge in the tetrahedral layer.

Expansion with glycerol (GLY)

The charge characteristics and basal spacings of GLY-solvated samples are given in Table 2. Four stages were observed: two homogeneous stages with basal spacings of about 18 Å and 14 Å, and two intermediate stages between 18 Å and 14 Å and between 14° and 10° (collapsed layer). Except for the beidellite samples (BS-3 and B2), the Na-saturated samples showed integral reflections with a basal spacing of about 18 Å. This suggests that a bilayer GLY-smectite complex has formed (Brindley, 1966). In the beidellite samples, a double EG-layer expanded phase in sample BS-3 and an intermediate stage between 18 Å and 14 Å in sample B2 were observed. The integral reflections with a basal spacing of 14 Å suggest that a monolayer GLY-smectite complex forms (Brindley, 1966).

Integral reflections with a basal spacing of about 14 Å were obtained for the K-saturated N1 and Ts samples. The asymmetrical reflections with a basal spacing between 14 Å and 18 Å or between 14 Å and 10 Å (collapse phase) were observed for the other K-saturated samples. The glycolated samples with a high total charge and a high proportion of tetrahedral charge showed nonintegral reflections with basal spacings between 14 Å and 10 Å.

The GLY-solvated, Ca-saturated samples, except for the sample BS-3, showed an integral series of reflections with basal spacings of about 17.7–17.9 Å. The basal spacing of Ca-saturated samples gradually decreases with increasing value of net layer charge. The d_{001} spacing of Ca-saturated samples with two EG-layers is smaller than that of Na-saturated samples. The BS-3 sample has two GLY-expanded phases with basal spacings of 17.37 Å and 14.58 Å and an integral series of reflections.

Expansion with water

The variations in basal spacings upon hydration of Na-, K- and Ca-saturated samples at different RHs are represented in Tables 3, 4, and 5. With Na-saturated samples (Table 3), the d_{001} spacing increases with increasing RH in distinct steps. All samples, except for N1, give a completely collapsed phase with a basal spacing of 9.8–10.0 Å at 0% RH. With increasing RH, an integral series of reflections with basal spacings of 12.4 Å and 15.6 Å appears. These states have a basal spacing of about 10.0 Å, 12.4 Å, and 15.6 Å and correspond to the dehydrated (0-water layer), the one-water layer hydrate, and the two-water layer hydrate, respectively. Three homogeneous states characterized by an integral series of reflections were observed in the range 0–90% RH. In this range, only a small difference in basal spacing was observed between homogeneous states of hydration. At the transition, integral reflections with long spacings, asymmetrical reflections, and doublet reflections were observed. There are various types of interstratified structures: regular, for sample SWy-1 in the range of 30–60% RH, and random- or segregation-type. Moore and Hower (1986) also reported regular interstratification between two hydrate states in Na-smectite. Therefore, in the range of 0–90% RH, it is probably difficult to evaluate any relationship between the crystallochemical properties and the expansion behavior. At 100% RH, most of these samples rapidly expanded further to a thickness equivalent to three-water layers with a d_{001} of about 18.5–19.0 Å,

https://doi.org/10.1346/CCMN.1992.0400111 Published online by Cambridge University Press

Table 3. Basal spacings (Å) of Na-saturated samples at various relative humidity conditions.

RH (%)	NG-1	SWy-1	N1	TU6	Sta-9c	Ts	M6	BS-3	SAz-1	B2
0	9.86	9.76	(11.63)	9.91	10.28	9.74	10.00	9.81	9.81	9.77
10	9.87	9.80	(11.95)	10.00	(10.65)	9.74	(10.78)	9.81	9.83	9.76
20	(10.78)	9.80	(12.63)	10.22	(11.79)	(10.16)	(11.79)	(10.92)	(11.48)	(10.65)
30	(12.11)	(10.53)	12.96	(12.28)	12.63	(10.63)	12.46	(12.37)	(12.45)	(11.79)
40	12.64	[11.19]	12.94	12.54	(13.39)	12.47	12.52	12.51	12.57	(12.28)
50	12.80	[11.79]	12.97	12.60	(13.81)	12.62	12.51	12.51	12.70	12.41
60	(13.81)	[12.45]	(13.81)	(14.03)	(14.98)	(14.62)	(14.03)	12.51	(13.81)	12.45
70	14.73	[15.24]	(14.49)	15.19	15.78	15.54	(14.49)	(13.60)	(14.98)	(12.81)
80	15.64	15.70	15.60	15.47	16.07	15.73	15.45	(14.98)	15.47	(14.03)
90	15.78	15.81	16.02	15.48	16.37	15.77	15.65	15.27	15.66	(14.98)
100	(18.41)	(23.25)	18.97	18.75	18.41	18.71	18.73	15.43	18.41	15.24

Values in parentheses are obtained from only (001) reflection of nonintegral series.
Values in brackets indicate the nonintegral series with reflection for long spacing.

while samples BS-3 and B2 remained with only two-water layers. Moreover, sample SWy-1 expanded to a thickness of more than three-water layers, while sample N1 expanded to only three-water layers. Whereas the pairs of samples SAz-1 and BS-3, B2 and SWy-1 and N1 have a similar layer charge, their expansion properties are different. In both cases, the spacings of the samples with negative charge dominantly in the octahedral sites gave larger basal spacings. These results suggest that the differences in expansion of these samples can be attributed to charge location.

With K-saturated samples (Table 4), the d_{001} spacings increase with increasing RH in distinct steps. All samples give a completely collapsed phase with a basal spacing of 10.2–10.6 Å at 0% RH. As the RH increases, an integral series of reflections with a basal spacing of about 12.4 Å appears. Two homogeneous states characterized by an integral series of reflections were observed in the range of 0–90% RH. In this range, little difference was observed during the transition between two homogeneous states of hydration. However, the relationship between the crystallochemical properties and the expansion behavior is not as simple as in the case of the Na-saturated samples. At 100% RH, samples SWy-1, N1, and Sta-9c expanded to a thickness of more than one-water layer, while most of the selected samples remained with one-water layer. Moreover, sample SWy-1 expanded to a thickness equivalent to two-water layers.

Except for sample SWy-1, integral reflections were obtained for the Ca-saturated samples (Table 5) between 30% and 80% RH. In this range, the basal spacings gradually increased from 14.5 to 16.0 Å. At 0% RH, the following phases were obtained: a phase characterized by an integral series of reflections with basal spacing of about 11.6 Å (samples SWy-1, TU6, M6, BS-3, and B2); a phase characterized by nonintegral and asymmetrical reflections (NG-1, N1 and Sta-9c); and a double-expanded phase with basal spacings of 11.6 Å and 13.5 Å and with an integral series of reflections (Ts and SAz-1). The 11.6 Å phase was comparable to one-water layer hydrated, Mg-vermiculite (Walker, 1956). According to Walker (1956), the 13.5 Å phase still has two-water layers between the silicate layers, but fewer water molecule sites are occupied than in the 14.36 Å phase. In sample BS-3, a 12.36 Å phase with an integral series of reflections was observed at 10% RH. With respect to this phase, no one has suggested an arrangement for the water molecules in the interlayer region. At 100% RH, most of these samples rapidly expanded further to a thickness equivalent to three-water layers with a d_{001} of about 18.5–19.5 Å, while samples BS-3 and B2 showed two-water layer hydrate with basal spacings of 15.5 Å and 18.6 Å and

Table 4. Basal spacings (Å) of K-saturated samples at various relative humidity conditions.

RH (%)	NG-1	SWy-1	N1	TU6	Sta-9c	Ts	M6	BS-3	SAz-1	B2
0	10.24	10.15	10.38	10.24	10.35	10.27	10.27	10.61	10.27	10.23
10	10.22	10.15	10.43	10.28	10.37	10.27	10.30	10.67	10.33	10.23
20	10.23	10.15	(11.48)	(10.78)	10.43	10.30	10.80	(12.11)	(11.33)	(11.19)
30	10.26	10.18	(12.11)	(11.63)	(11.33)	(11.19)	(11.95)	(12.28)	(11.95)	(11.63)
40	(11.63)	(11.19)	(12.28)	12.56	(11.95)	(11.95)	(12.28)	(12.28)	(12.28)	(11.95)
50	(11.79)	(11.63)	12.73	12.62	12.73	12.44	(12.45)	12.54	12.43	(11.95)
60	(11.95)	(11.95)	12.80	12.66	12.82	12.60	(12.45)	12.56	12.49	(11.95)
70	(11.95)	12.26	12.89	12.64	12.92	12.60	12.69	12.56	12.56	(11.95)
80	12.67	12.46	12.99	12.69	12.92	12.65	12.73	12.56	12.59	(11.95)
90	12.77	(13.81)	(13.39)	12.69	13.00	12.71	12.75	12.62	12.59	(11.95)
100	12.77	15.92	(13.81)	12.73	(13.60)	12.77	12.75	12.62	12.59	(11.95)

Values in parentheses are obtained from only (001) reflection of nonintegral series.

https://doi.org/10.1346/CCMN.1992.0400111 Published online by Cambridge University Press

Table 5. Basal spacings (Å) of Ca-saturated samples at various relative humidity conditions.

RH (%)	NG-1	SWy-1	N1	TU6	Sta-9c	Ts	M6	BS-3	SAz-1	B2
0	(10.78)	11.34	(13.00)	11.82	(12.28)	11.55* 13.48*	11.66	11.78	11.66* 13.35*	11.78
10	12.44	(12.63)	(13.60)	(13.00)	(13.60)	(13.19)	(13.00)	12.36	(13.60)	12.34
20	(13.60)	(13.60)	14.35	14.61	14.88	14.84	14.80	(13.60)	14.95	(14.26)
30	15.15	(14.49)	14.68	14.93	15.18	15.09	14.95	15.05	15.15	15.00
40	15.29	15.16	14.89	15.12	15.37	15.22	15.11	15.13	15.30	15.13
50	15.42	15.50	15.21	15.26	15.51	15.36	15.23	15.16	15.36	15.21
60	15.48	15.62	15.25	15.35	15.65	15.49	15.40	15.28	15.44	15.21
70	15.63	15.64	15.57	15.55	15.75	15.67	15.48	15.31	15.56	15.34
80	15.68	15.74	15.75	15.78	15.94	15.77	15.54	15.34	15.76	15.38
90	15.91	15.90	15.94	15.87	16.07	(16.99)	15.92	15.44	15.87	15.41
100	18.43	19.49	19.06	18.91	19.11	18.96	18.92	15.50	18.65	15.52

Values in parentheses are obtained from only (001) reflection of nonintegral series.
Asterisks indicate the subordinate reflections for doubly-expanded phases having different spacings.

an integral series of reflections. Whereas samples SAz-1, BS-3, and B2 have a similar layer charge, their expansion properties are different. In this case, the spacings of the tetrahedrally-charged samples BS-3 and B2 are smaller than those of the octahedrally-charged sample SAz-1. The results suggest that differences in the expansion of these samples can be attributed to an effect of charge location.

Marked differences in expansion behavior were obtained for each sample at 100% RH. Under lower RH conditions, a small difference was observed in the transition between the two homogeneous states of hydration. However, it is difficult to determine any relationship between crystallochemical properties and expansion behavior from this difference. It is necessary to consider the types of interstratified structures and the proportions of the component layers in determining any relationship because there are various types of interstratified structures at the transition. In the hydration range 0–90% RH, charge distribution is a significant factor. On the other hand, phase changes from 90% to 100% RH are rapid. Clearly the net layer charge and charge location affect the changes between the hydrated phases from 90% to 100% RH.

Expansion properties vs amount and location of layer charge

According to current theory, interlayer solvation (or hydration) exerts a repulsive force between the silicate layers and leads to expansion. On the other hand, if electrostatic attractive forces between the negatively-charged silicate layers and the positively-charged interlayer cations dominate, then the repulsive forces do not lead to expansion. Therefore, the expansion reaction is determined by a balance between the opposing forces. In comparing the expansion properties to the amount and location of layer charge for each sample, the repulsive forces can be regarded as constant for the following reasons: (1) homoionic samples were investigated under the same conditions, (2) the negatively-charged silicate layers moved apart from one another to some extent.

The main attractive force in the expansion is due to electrostatic interactions between the interlayer cations and the negatively-charged silicate surface. The positively- and negatively-charged sites can be treated as point charges. The attraction energy, Er, is given by the Coulomb electrostatic energy. The general formulation of the energy is given by:

$$\mathrm{Er} = \frac{q_i \cdot q_s}{\epsilon \cdot r}, \qquad (1)$$

where q_i and q_s are the charges in the interlayer and the silicate layer, respectively; r is the distance between q_i and q_s; and ϵ is the dielectric constant. Hawel and Licastro (1961) found that the dielectric constant of a clay crystal itself was 5 or 6. Keren and Shainberg (1975) used a value of 5 for the calculation of energy change in the hydration of montmorillonite. A value of 5 has been used for the dielectric constant in the calculations here. In the expansion, from an expanded state (*e*-state) to a further expanded state (*f*-state), the energy ("*expansion energy*") required to push the silicate layers apart is given by:

$$\Delta\mathrm{Er} = \mathrm{Er}_e - \mathrm{Er}_f, \qquad (2)$$

where Er_e and Er_f are the attraction energies in the *e*-state and *f*-state, respectively.

As mentioned above, differences in the expansion of smectites with the same layer charge and under the same hydration and solvation conditions can be attributed to an effect of charge location. In the calculation of the ΔEr value, the charge location must be considered. In considering the effects of charge location, r is the distance between the interlayer cation and the negative charge, r_t is the distance between the interlayer cation and the negative charge on the tetrahedral layer, and r_o is the distance between the inter-

https://doi.org/10.1346/CCMN.1992.0400111 Published online by Cambridge University Press

Table 6. Values of distance (Å) r_t and r_o used for calculation of ΔEr.

	1-EG layer	2-EG layers	1-GLY layer	2-GLY layers	1-W layer	2-W layers	3-W layers
r_t	3.72	5.22	3.87	5.72	2.92	4.52	6.12
r_o	5.93	7.43	6.08	7.93	5.13	6.73	8.33

layer cation and the negative charge on the octahedral layer. Consequently, ΔEr is given by:

$$\Delta Er = Er_e - Er_f = \left(\frac{q_i \cdot q_t}{\epsilon \cdot r_{te}} + \frac{q_i \cdot q_o}{\epsilon \cdot r_{oe}}\right) - \left(\frac{q_i \cdot q_t}{\epsilon \cdot r_{tf}} + \frac{q_i \cdot q_o}{\epsilon \cdot r_{of}}\right), \quad (3)$$

where r_{te} and r_{oe} are the distances between the interlayer cations and the tetrahedral and octahedral charges in the *e*-state, respectively; and r_{tf} and r_{of} are the distances between the interlayer cations and the tetrahedral and octahedral charges in the *f*-state, and q_t and q_o are the charge on the tetrahedral and octahedral layers, respectively. We assumed that the position of negative charge due to isomorphic substitution in silicate layers is distributed over at least the three surface oxygens coordinated to tetrahedral Al^{3+}, or over at least the ten surface oxygens of the four silicon-oxygen tetrahedra linked to the sites of octahedral substitution (according to Farmer and Russell, 1971), and the cations are centered in the interlayer region. The values for r_t and r_o are given in Table 6. The *expansion energies* calculated from formula (3) are presented in Table 7. The ΔEr can be treated as a quantitative indicator of expansion properties, although the value of ΔEr does not have a physical meaning.

The relationships between the basal spacings with various solvations and hydration (at 100% RH) treatments, and the ΔEr for each expansion treatment are presented in Figures 2, 3, and 4. No significant differ-

Table 7. *Expansion energy* ΔEr (kcal/mol) in the expansion process of samples after various treatments.

Sample	ΔEr (kcal/mol)			
	EG_{1-2}	GLY_{1-2}	W_{1-2}	W_{2-3}
SWy-1	1.358	1.505	1.964	1.088
N1	1.592	1.750	2.370	1.247
NG-1	2.876	3.115	4.499	2.160
TU6	2.549	2.784	3.880	1.960
Sta-9c	1.722	1.936	2.362	1.435
Ts	2.283	2.544	3.246	1.855
M6	2.591	2.873	3.748	2.077
BS-3	6.050	6.559	9.431	4.557
SAz-1	3.396	3.791	4.794	2.774
B2	5.613	6.123	8.577	4.302

EG_{1-2} and GLY_{1-2} are the *expansion energy* from one-layer to two-layer solvated state of ethylene glycol and glycerol complexes, respectively. W_{1-2} and W_{2-3} are the *expansion energy* from one-layer to two-layer hydrated state and from two-layer to three-layer hydrated state, respectively.

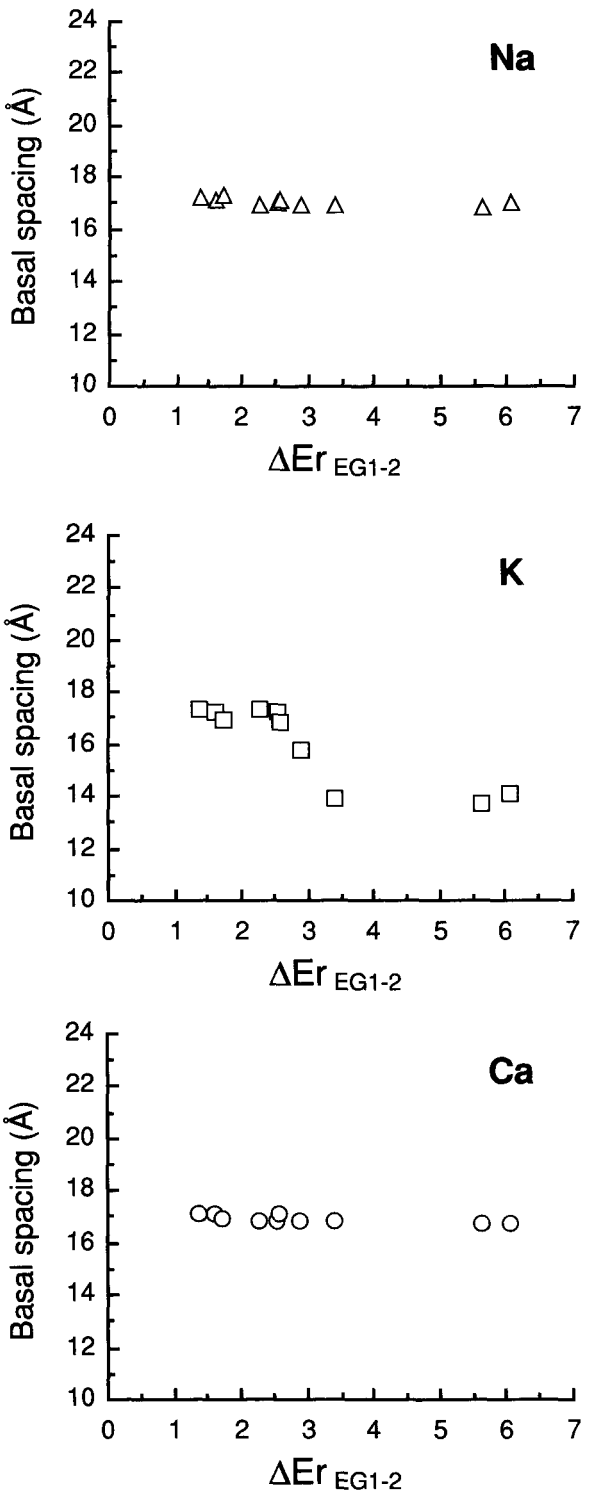

Figure 2. Relationship between the *expansion energy* ΔEr (kcal/mol) and basal spacing of homoionic samples after solvation with ethylene glycol.

https://doi.org/10.1346/CCMN.1992.0400111 Published online by Cambridge University Press

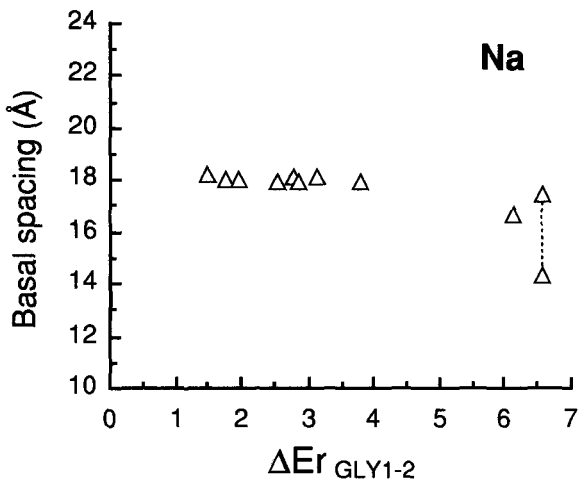

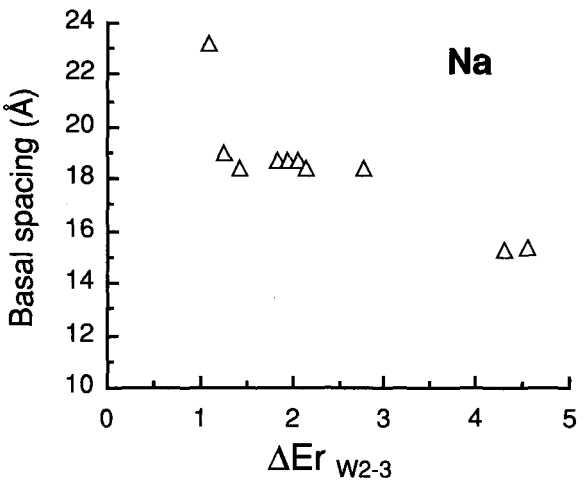

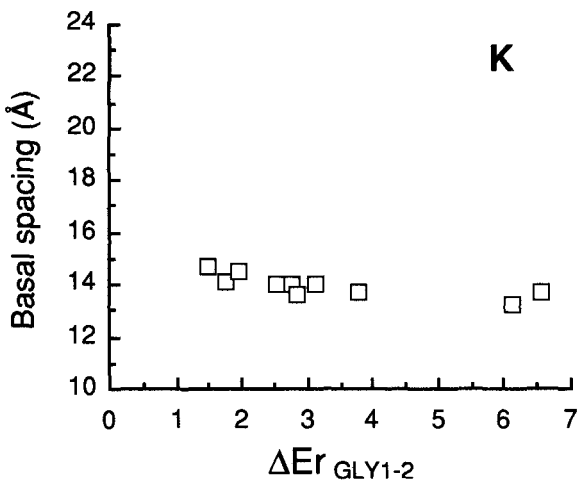

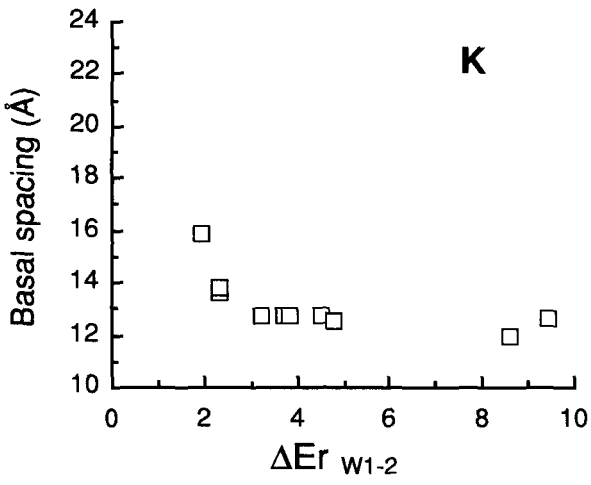

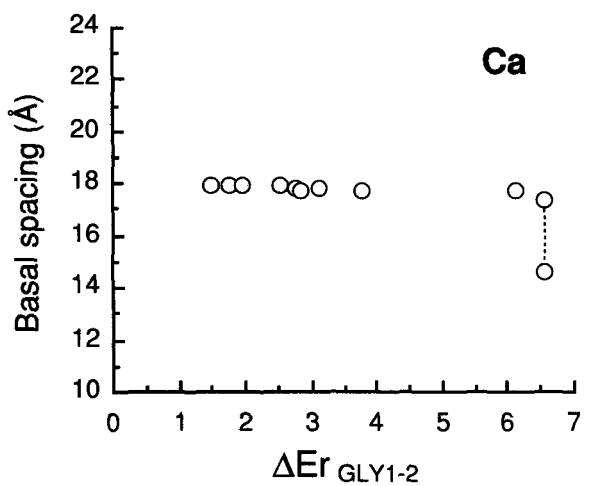

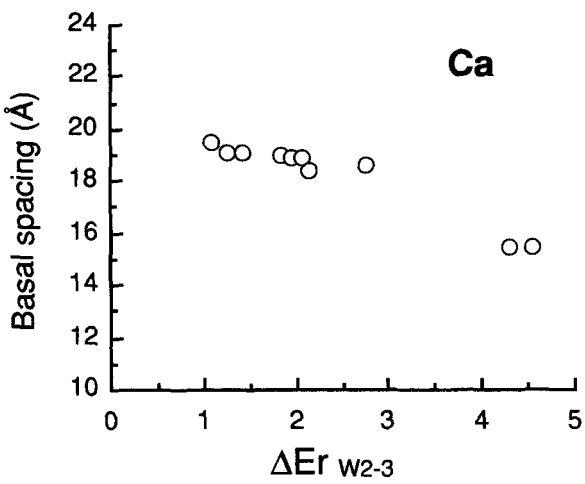

Figure 3. Relationship between the *expansion energy* ΔEr (kcal/mol) and basal spacing of homoionic samples after solvation with glycerol. Open symbol joined by a broken line; subordinate reflections for double-expanded phases having different spacings.

Figure 4. Relationship between the *expansion energy* ΔEr (kcal/mol) and basal spacing of homoionic samples at 100% RH.

https://doi.org/10.1346/CCMN.1992.0400111 Published online by Cambridge University Press

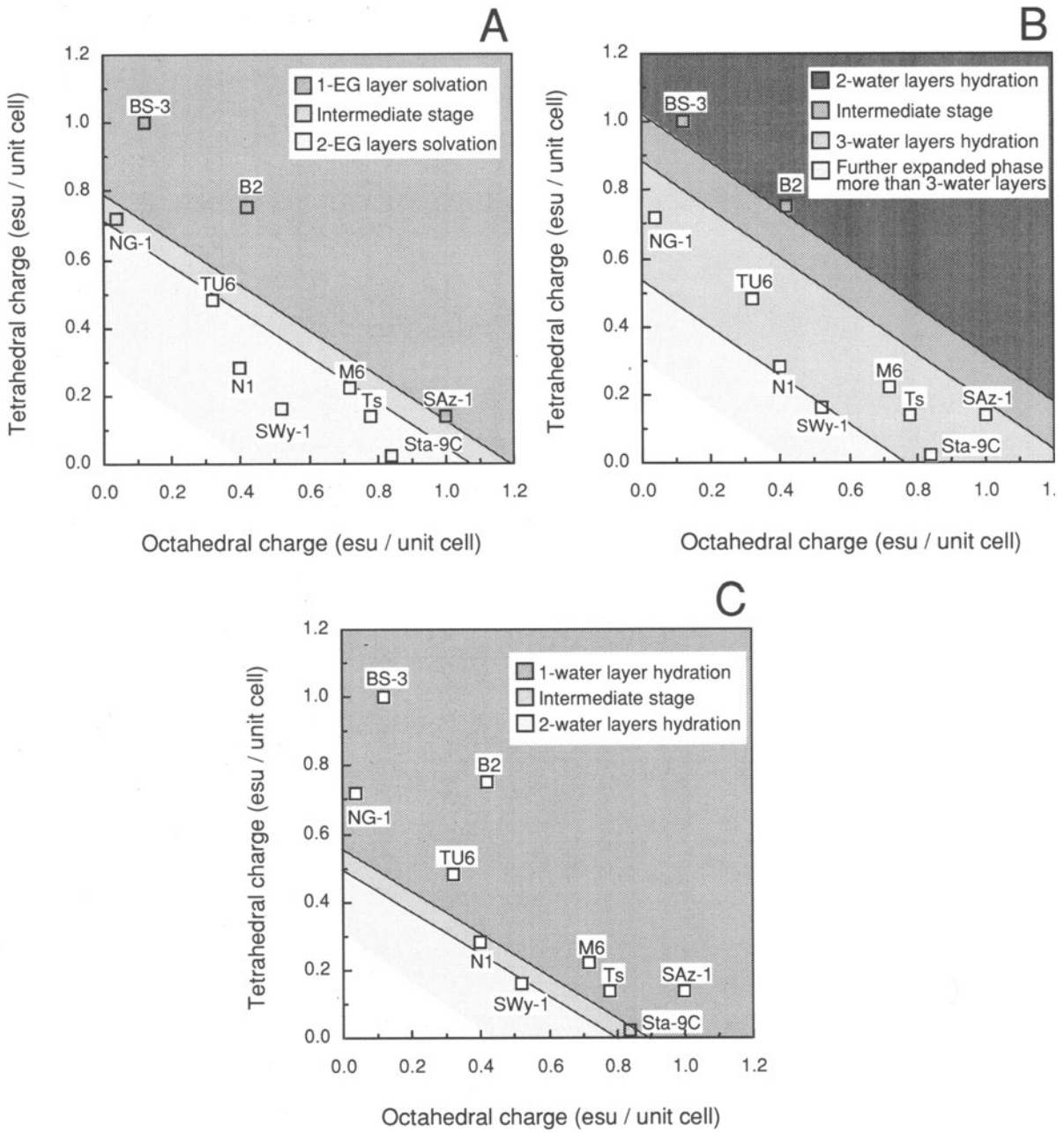

Figure 5. Relationship between the expanded phase and the charge characteristic. (A) K-samples with EG-solvation. (B) Na-samples at 100% RH. (C) K-samples at 100% RH.

ence in basal spacings was found for glycerol-solvated, K-saturated smectites. Similarly, EG-solvated Na- and Ca-saturated samples afforded no clear differentiation of smectites (Figure 2). However, the basal spacings of other treated samples are apt to contract stepwise with increasing value of ΔEr. The data presented in Figures 2, 3, and 4 suggest that the lower energy required to push the silicate layers apart results in larger basal spacings, and a higher energy prevents further expansion of the layers. There is a relationship between the ΔEr values and expansion. Clearly, the effects of the amount and location of layer charge are represented by the ΔEr term.

Suggested method for characterization of layer charge

As shown in Figures 2, 3, and 4, the large differences in the basal spacings of the smectites are observed for K-samples with EG-solvation, and Na- and K-saturated samples at 100% RH. The experimental boundaries of the expanded phases lie at approximately 2.6

https://doi.org/10.1346/CCMN.1992.0400111 Published online by Cambridge University Press

and 3.2 kcal/mol for EG-solvated K-samples; 1.1, 3.0, and 4.0 kcal/mol for Na-saturated samples at 100% RH; and 2.0 and 2.5 kcal/mol for Na-saturated samples at 100% RH. For these samples, the figures showing the relationship between each expanded phase and the charge characteristics are obtained on the basis of the isoquants of ΔErs, given the boundary of expanded phases (Figure 5). The isoquants of ΔErs with solid lines are obtained from Eq. (3) for each ΔEr.

With the present characterization method (expanded behavior test), the identification of the expandable clay minerals is generally based on the expanding behavior of minerals saturated with Mg and solvated with either ethylene glycol or glycerol (Walker, 1958; Harward *et al.*, 1969) and on the collapsing behavior of K-saturated minerals (Weaver, 1956). These expanding-behavior tests have been widely used for distinguishing smectites from vermiculites. These tests are not suggestive for the characterization of layer charge in common smectites with continuous characters of charge. However, the expansion-behavior test is applied to all common smectites because the layer charge of all smectites can plot within Figure 5. The Greene-Kelly test can estimate the relative proportion of octahedral or tetrahedral charge by comparison of the observed and calculated X-ray diffraction patterns. Therefore, the behavior test using these figures may be combined with the Greene-Kelly test to estimate the amount and the location of the layer charge of common smectites.

ACKNOWLEDGMENTS

The authors are grateful to Dr. T. Oba, Joetsu University of Education, for valuable suggestions and encouragement. Special acknowledgments are due to Dr. H. Kodama of Land Resource Research Centre of Canada and Dr. T. Iwasaki of Government Industrial Research Institute, Tohoku for valuable suggestions and critical reading. The authors also wish to thank the following for contributing samples: Emeritus Prof. K. Nagasawa of Shizuoka University (Ts), Prof. S. Aoki of Toyo University (Sta-9c), Assoc. Prof. T. Matsuda of Okayama University (BS-3), and Dr. M. J. Wilson of the Macaulay Institute for Soil Research (B2).

REFERENCES

Aoki, S., Kohyama, N., and Sudo, T. (1974) An iron-rich montmorillonite in sediment core from the northeastern Pacific: *Deep-Sea Res.* **21,** 865–875.

Brindley, G. W. (1966) Ethylene glycol and glycerol complexes of smectites and vermiculites: *Clay Miner.* **6,** 237–259.

Brown, G. and Farrow, R. (1956) Introduction of glycerol into flake aggregates by vapor pressure: *Clay Miner. Bull.* **3,** 44–45.

Brunton, G. (1955) Vapor glycolation: *Amer. Mineral.* **40,** 124–126.

Farmer, V. C. and Russell, J. D. (1971) Interlayer complexes in layer silicates: *Trans. Faraday Soc.* **67,** 2737–2749.

Glaeser, R. and Mering, J. (1968) Homogeneous hydration domains of the smectites: *C.R. Acad. Sci., Paris* **46,** 436–466.

Greene-Kelly, R. (1953a) Irreversible dehydration in montmorillonite. Part II: *Clay Miner. Bull.* **2,** 52–56.

Greene-Kelly, R. (1953b) The identification of montmorillonoids in clays: *J. Soil Sci.* **4,** 233–237.

Greene-Kelly, R. (1955) Dehydration of montmorillonite minerals: *Miner. Mag.* **30,** 604–615.

Harward, M. E. and Brindley, G. W. (1965) Swelling properties of synthetic smectite in relation to lattice substitutions: *Clays & Clay Minerals* **13,** 209–222.

Harward, M. E., Carstea, D. D., and Sayegh, A. H. (1969) Properties of vermiculites and smectites: Expansion and collapse: *Clays & Clay Minerals* **16,** 437–447.

Hawel, B. F. and Licastro, P. H. (1961) Dielectric behavior of rocks and minerals: *Amer. Mineral.* **46,** 269–288.

Horváth, I. and Novák, I. (1976) Potassium fixation and the charge of montmorillonite layers: *Proc. Int. Clay Conf., Mexico City, 1975,* S. W. Bailey, ed., Applied Publishing, Wilmette, Illinois, 185–189.

Iwasaki, T. (1979) Relationship between X-ray basal reflections and interlayer cations of montmorillonite: On the distribution of Ca and Na ions: *J. Miner. Soc. Japan, Spec. Issue* **14,** 78–89 (in Japanese with English abstract).

Iwasaki, T. and Watanabe, T. (1988) Distribution of Ca and Na ions in dioctahedral smectites and interstratified dioctahedral mica/smectites: *Clays & Clay Minerals* **36,** 73–82.

Jaynes, W. F. and Bigham, J. M. (1987) Charge reduction, octahedral charge, and lithium retention in heated, Li-saturated smectites: *Clays & Clay Minerals* **35,** 440–448.

Jenkins, H. D. B. and Hartman, P. (1979) A new approach to electrostatic energy relations in minerals: The dioctahedral and trioctahedral micas: *Phil. Trans. Roy. Soc.* **A293,** 169–208.

Jenkins, H. D. B. and Hartman, P. (1982) A new approach to electrostatic calculations for complex silicate structures and their application to vermiculites containing a single layer of water molecules: *Proc. Int. Clay Conf., Bologna, Pavia, 1981,* H. van Olphen and F. Veniale, eds., Elsevier, Amsterdam, 87–95.

Keren, R. and Shainberg, I. (1975) Water vapor isotherms and heat of immersion of Na/Ca-montmorillonite systems—I: Homoionic clay: *Clays & Clay Minerals* **23,** 193–200.

Kodama, H., Ross, G. J., Iiyama, J. T., and Robert, J-L. (1974) Effect of layer charge location on potassium exchange and hydration of micas: *Amer. Mineral.* **59,** 491–495.

Machajdik, D. and Čičel, B. (1981) Potassium and ammonium-treated montmorillonites. II. Calculation of characteristic layer charge: *Clays & Clay Minerals* **29,** 47–51.

Malla, P. B. and Douglas, L. A. (1987) Layer charge properties of smectites and vermiculites: Tetrahedral vs. octahedral: *Soil Sci. Soc. Amer. J.* **51,** 1362–1366.

Matsuda, T. (1988) Beidellite from the Sano mine, Nagano Prefecture, Japan: *Clay Sci.* **7,** 151–159.

Mooney, R. W., Keenan, A. G., and Wood, L. A. (1952) Adsorption of water vapor by montmorillonite. II. Effect of exchangeable ions and lattice swelling as measured by X-ray diffraction: *J. Amer. Chem. Soc.* **74,** 1331–1374.

Moore, D. M. and Hower, J. (1975) Ordered interstratification of dehydrated and hydrated Na-smectite: *Clays & Clay Minerals* **34,** 379–384.

Nadeau, P. H., Farmer, V. C., McHardy, W. J., and Bain, D. C. (1985) Compositional variations of the Unterrupsroth beidellite: *Amer. Mineral.* **70,** 1004–1010.

Nagasawa, K. (1988) Study on a behavior of water in heating of clay minerals: *Report of grant-aid for science research* (**NO.61420016**), Ministry of Education, Japan, 1–10 (in Japanese).

Schultz, L. G. (1969) Lithium and potassium adsorption; Dehydroxylation and structural water content of aluminous smectites: *Clays & Clay Minerals* **17,** 115–149.

Suquet, H., De la Calle, C., and Pezerat, H. (1975) Swelling and structural organization of saponite: *Clays & Clay Minerals* **23,** 1–9.

Suquet, H., Iiyama, J. T., Kodama, H., and Pezerat, H. (1977) Synthesis and swelling properties of saponites with increasing layer charge: *Clays & Clay Minerals* **25,** 231–242.

Walker, G. F. (1956) The mechanism of dehydration of Mg-vermiculite: *Clays & Clay Minerals* **4,** 101–115.

Walker, G. F. (1958) Reactions of expanding-lattice clay minerals with glycerol and ethylene glycol: *Clay Miner. Bull.* **3,** 302–313.

Watanabe, T. (1981) Identification of illite/montmorillonite interstratification by X-ray powder diffraction: *J. Miner. Soc. Japan, Spec. Issue* **15,** 32–41 (in Japanese).

Watanabe, T. and Sato, T. (1988) Expansion characteristics of montmorillonite and saponite under various relative humidity conditions: *Clay Sci.* **7,** 129–138.

Weaver, C. E. (1956) The distribution and identification of mixed layer clays in sedimentary rocks: *Amer. Mineral.* **41,** 202–221.

(Received 23 April 1991; accepted 4 November 1991; Ms. 2093)